Acta Oceanol. Sin., 2017, Vol. 36, No. 6, P. 95–103
DOI: 10.1007/s13131-017-1046-7
http://www.hyxb.org.cn
E-mail: hyxbe@263.net

Distribution of reactive aluminum under the influence of mesoscale eddies in the western South China Sea

LIU Jiaxing[1, 2, 3], ZHOU Linbin[1, 2], TAN Yehui[1, 2], WANG Qiong[1, 2, 3], HU Zifeng[1, 2, 3], LI Jiajun[1, 2, 3], JIANG Xin[1, 2, 3], KE Zhixin[1, 2*]

[1] Key Laboratory of Tropical Marine Bio-resources and Ecology, South China Sea Institute of Oceanology, Chinese Academy of Sciences, Guangzhou 510301, China

[2] Guangdong Provincial Key Laboratory of Applied Marine Biology, South China Sea Institute of Oceanology, Chinese Academy of Sciences, Guangzhou 510301, China

[3] University of Chinese Academy of Sciences, Beijing 100049, China

Received 7 March 2016; accepted 30 June 2016

Abstract

To understand the distribution of aluminum (Al) under the influence of mesocale eddies in the western South China Sea (SCS), sea level anomaly, geostrophic current, environmental parameters and reactive Al were investigated in the western SCS in August 2013. The highest reactive Al concentration ((180±64) nmol/L) was observed in the surface waters, indicating a substantial atmospheric input. Vertically, the reactive Al decreased from the surface high concentration to the subsurface minima at the depth of chlorophyll *a* (Chl *a*) maxima and then increased again with depth at most of the stations. The average concentration of reactive Al in the upper 100 m water column was significantly lower in the cyclonic eddy ((137±6) nmol/L) as compared with that in the non-eddy waters ((180±21) nmol/L). By contrast, the average concentrations of Chl *a* and silicate in the upper 100 m water column were higher in the cyclonic eddy and lower in the anticyclonic eddy. There was a significant negative correlation between the average concentrations of reactive Al and Chl *a* in the upper 100 m water column. The vertical distribution of reactive Al and the negative correlation between reactive Al and Chl *a* both suggest that the reactive Al in the upper water column was significantly influenced by biological removal processes. Our results indicate that mesoscale eddies could regulate the distribution of reactive Al by influencing the primary production and phytoplankton community structure in the western SCS.

Key words: reactive aluminum, mesoscale eddy, chlorophyll *a*, biological removal, phytoplankton, primary production, western South China Sea

Citation: Liu Jiaxing, Zhou Linbin, Tan Yehui, Wang Qiong, Hu Zifeng, Li Jiajun, Jiang Xin, Ke Zhixin. 2017. Distribution of reactive aluminum under the influence of mesoscale eddies in the western South China Sea. Acta Oceanologica Sinica, 36(6): 95–103, doi: 10.1007/s13131-017-1046-7

1 Introduction

Aluminum (Al) is the most abundant metallic element in the earth's crust (Taylor, 1964). The distribution of Al in the ocean represents a potent geochemical tracer of terrigenous input to the ocean (Orians and Bruland, 1986; Measures and Vink, 2000; Measures et al., 2005; Giesbrecht et al., 2013). Al distribution in seawater is associated with biological activity (such as biological uptake, and passive adsorption on biogenic particle surface), but to date no established biological function of Al has been found (Dammshäuser et al., 2011). For a better understanding of the roles of Al in the marine biogeochemical cycle, it is important to investigate the distribution of Al in the oceans.

Atmospheric input is the main source of Al in the surface of open oceans (Duce et al., 1991; Measures and Vink, 2000; Kramer et al., 2004; Measures et al., 2015). Typically, the scavenging type of vertical distribution of dissolved Al in the Pacific and Atlantic Oceans is characterized with the highest concentration in the surface waters mainly caused by atmospheric dust input, and a mid-depth minimum due to particle scavenging, and an increase by remineralization in bottom waters (Orians and Bruland, 1986; Measures and Edmond, 1990; Hydes et al., 1988; Chou and Wollast, 1997; Schüßler et al., 2005; Tria et al., 2007). Al in seawater could be removed by either passive or active biological processes (Orians and Bruland, 1986) such as adsorption onto biogenic particles or active incorporation into phytoplankton cell tissues (Stoffyn, 1979; Moran and Moore, 1988; Gehlen et al., 2002; Li et al., 2013; Wang et al., 2013). Significant positive correlation between biological productivity and the removal of Al in the Atlantic Ocean (Dammshäuser et al., 2013), the English Channel (Hydes, 1989) and the southern Yellow Sea (Ren et al., 2011) have been reported. In addition to the biological removal, physical processes (such as mesoscale eddy) and chemical (such as chemical precipitation) processes are also important factors influencing Al distribution in seawater (Stoffyn and Mackenzie, 1982; Brown et al., 2012; Measures et al., 2015).

Mesoscale eddies play a critical role in marine biogeochem-

Foundation item: The Strategic Priority Research Program of the Chinese Academy of Sciences under contract No. XDA11020305; the National Basic Research Program (973 program) of China under contract No. 2015CB452903; the Special Fund for Agro-scientific Research in the Public Interest under contract No. 201403008; the National Project of Basic Sciences and Technology under contract No. 2017FY201404; the National Natural Science Foundation of China under contract Nos 41506150 and 41276162.
*Corresponding author, E-mail: kzx@scsio.ac.cn

istry by affecting water mass mixing, nutrient supply, primary production and efficiency of the biological carbon pump in the upper oceans (Benitez-Nelson et al., 2007). Cyclonic eddies can result in upwelling, and an uplift of the thermocline and nutricline; on the contrary, downwelling often occurs in the anticyclonic eddies (McGillicuddy et al., 1998). Mesoscale eddies provides an ideal natural laboratory for investigating the relationship between eddy-affected biological production and the distribution of trace metals. Although Gelado-Caballero et al. (1996) and Brown et al. (2012) demonstrated that mesoscale eddy could affect the distribution of Al by affecting the movement of water mass in the Central East Atlantic waters and in the northern Gulf of Alaska, respectively, to date no established publication has reported the link between the distribution of Al and mesoscale eddy in the South China Sea (SCS).

The SCS is located in the subtropical and tropical western Pacific. The upper water column is permanently stratified, and exhibits typical characteristics of an oligotrophic ocean. The upper layer circulation in the SCS is influenced by the seasonal reversing monsoon, and numerous mesoscale eddies are always persistently found in the SCS (Wang et al., 2003; Chow et al., 2008; Xiu et al., 2010). In summer, both cyclonic and anticyclonic eddies can exist in the deep basin of the western SCS (Xue et al., 2004; Wang et al., 2003). However, it is still unclear whether and how these processes could influence the distribution of Al in the SCS.

In this study, we investigated the distribution of reactive Al (sum of fraction of dissolved Al and fraction of labile "particulate Al") under the influence of mesoscale eddies in the western SCS based on the survey data of reactive Al, chlorophyll *a* (Chl *a*), silicate, seawater temperature and salinity, and the remote sensing data of sea level anomaly (SLA) and geostrophic current vectors. Our study indicate that mesoscale eddies could regulate the distribution of reactive Al by influencing the primary production and phytoplankton community structure in the western SCS.

2 Materials and methods

2.1 *Study area*

The survey was conducted from 9 to 29 August, 2013 in the western SCS (12.5°–17.0°N, 110.5°–114.0°E; Fig. 1). Thirty-five stations were investigated for the reactive Al, and biological and environmental parameters including Chl *a*, silicate, seawater temperature and salinity, and the remote sensing data of average SLA and geostrophic current vectors, covering two eddies being cyclonic and anticyclonic, respectively (Fig. 1a). The bottom depth of the stations ranged from 496 m to 4 423 m.

2.2 *Hydrographic data, sample collection and analysis*

Seawater samples were collected at six depths in the upper 200 m (5, 25, 50, 75, 100 and 200 m) using 5-L Niskin bottles assembled on a CTD (Seabird SBE 911) rosette sampler. The temperature and salinity data were collected from the CTD.

For measuring reactive Al, seawater from the Niskin bottles (Niskin bottles were thoroughly cleaned by soaking in diluted acid before the survey and were rinsed by Milli-Q water before every sampling) was directly dispensed into polyethylene bottles, which were rinsed three times with Milli-Q water until a neutral pH after soaked in HCl solution (2.5 mol/L) for a week. The samples were not filtered (Measures, 1999) and blanks (Milli-Q water) were prepared at sea. After collection, the samples were frozen at –20°C until analysis (Ren et al., 2001). In the laboratory, the frozen samples were thawed, and reactive Al in the sample was determined by fluorometry using the Al-lumogallion complexation method (Zhang et al., 2000; Ren et al., 2011). The accuracy and precision of the analyses (triplicate samples) were determined by measurements of Chinese reference materials (CRM, GSBG62006-90, Solution sample, National Research Center for Certified Reference Material), which showed a difference within 5% at 18 nmol/L. The reagent blank was lower than 3 nmol/L.

In previous works by Orians and Bruland (1986) and Ren et al. (2011), by filtering the seawater samples with filters with pore size of 0.2 μm or 0.45 μm, Al in the filtrate and on the filter were divided into dissolved and particulate forms, respectively. The dissolved Al samples should be acidified to pH 1.8–2.0 prior to analysis using the Al-lumogallion complexation method (Zhang et al., 2000; Ren et al., 2011). Fraction of Al in the particulate form that could be extracted by acetic acid (HAc, pH=2) was the "labile particulate Al" (Berger et al., 2008). Except the dissolved Al, fraction of labile particulate Al also might be influenced by biological

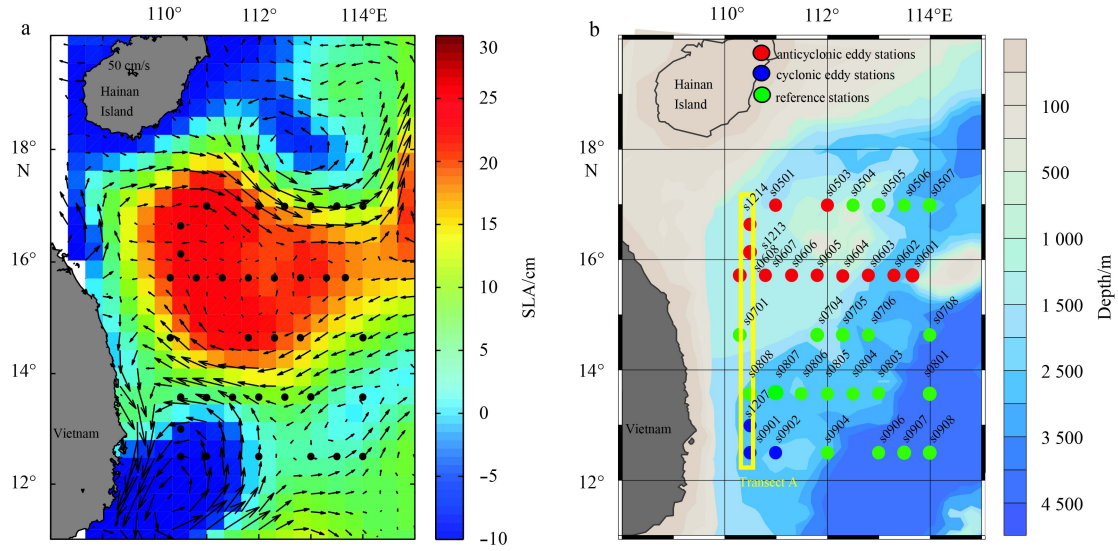

Fig. 1. Average sea level anomaly with overlaid geostrophic current vectors (a) and sampling stations in the western SCS during 9 to 29 August, 2013 (b). A north-south transect A was marked by the yellow lines.

activity, such as biological uptake, adsorption and aggregation processes on biogenic particle surfaces (Ren et al., 2011). In addition, the contaminants might be introduced into the sample along with using filtering techniques under shipboard conditions. Therefore, the water samples in this study were unfiltered and non-acidified. As adding HAc-NaAc (sodium acetic acid) buffer (pH=5) into the samples is an essential procedure by using the Al-lumogallion complexation method, the Al measured in the present study was actually reactive Al (Moore, 1981; Measures, 1999), which consisted of two fractions including fraction of the "dissolved Al" and fraction of the labile particulate Al.

For determination of Chl *a*, 500 mL seawater was filtered onto a Whatman GF/F glass fiber filter and stored at –20°C in the dark until determination. Chl *a* in the filters was completely extracted with 90% acetone (v/v) for 24 h at –20°C in the dark and then measured by fluorometry using a Turner Design 10-AU fluorometer (Parsons et al., 1984).

For silicate measurement, the seawater was decanted into a 100 mL polyethylene bottle, frozen immediately and stored at –20°C until analysis in the laboratory. According to the standard colorimetric techniques (Kirkwood et al., 1996), the concentrations of silicate were analyzed using a flow-injection autoanalyzer (Quickchem 8500, Lachat Instruments, USA).

The diffuse attenuation coefficient K_d (490), and photosyn thetically available radiation at the sea surface data with 4 km resolution were downloaded from http://oceancolor.gsfc.nasa.gov/. The integrated primary production was calculated using vertically generalized production model (VGPM) (Behrenfeld and Falkowski, 1997).

The near-real time daily SLA and surface geostrophic current with a high resolution of (1/3)°×(1/3)° were derived from merged and gridded products of TOPEX/Poseidon, Jason-1 and ERS-1/2 (http://www.aviso.oceanobs.com). Averaged SLA and surface geostrophic current during the survey period were used for the identifying of mesoscale eddies according to the criteria by Wang et al. (2003). On the basis of temperature, salinity and SLA data, the 35 stations were grouped into three types (cyclonic eddy, anticyclonic eddy and reference stations) according to the K-means cluster analysis (Fig. 1b).

3 Results

3.1 *Eddy characterization*

Two mesoscale eddies were identified in the study area on the basis of the SLA and surface geostrophic current data. One anticyclonic eddy was located in the north of the sampling area, while a cyclonic eddy occurred in the southern part of the sampling area (Fig. 1a). The maximum SLA (at Sta. S0501) was 28.9 cm for the anticyclonic eddy characterized by clockwise rotation of surface geostrophic currents. The minimum SLA (at Sta. S0901) for the cyclonic eddy was –6.16 cm. Stations S0901, S0902 and S1207 were apparently affected by the cyclonic eddy characterized with anticlockwise rotation of surface geostrophic currents.

3.2 *Characteristics of temperature and salinity in eddies and adjacent waters*

The cyclonic eddy stations were characterized by lower temperature ((18.58±0.48)°C) and higher salinity (34.32±0.05), while the anticyclonic eddy stations exhibited higher temperature ((22.68±0.64)°C) and lower salinity (34.03±0.05) as compared to the reference stations (*t*-test, $p<0.01$; Table 1). In addition, the isotherms and isohalines along the south-north Transect A (throughout the anticyclonic and cyclonic eddies; Fig. 1b) sank from Sta. S0701 to the northern Sta. S1214, and the sinking of the isotherms and isohalines were especially dramatic between the depth from 100 m to 200 m (Figs 2a and b). Compared with those in adjacent stations, the 20°C and 17.5°C isotherms near Sta. S1214 both sank by 50 m, and the 34.5 isohaline also sank by 50 m. The significant sinking of isotherms and isohalines indicate that Sta. S1214 was located at the anticyclonic eddy core. In contrast, the isotherms were significantly uplifted from Sta. S0701 toward the southern Sta. S0901. Both the 17.5°C and 20°C isotherms near Sta. S0901 rose by 50 m, and the 34.5 isohaline was also uplifted between the depth from 100 m to 50 m, indicating that Sta. S0901 was significantly affected by the cyclonic eddy characterized with upwelling (Figs 2a and b).

3.3 *Distributions of Chl a, integrated primary production and silicate*

Generally, Chl *a* concentration was low in the surface ((0.096±0.026) μg/L), and it reached to a maximum ((0.216±0.111) μg/L) in the subsurface and then decreased with the depth. Specifically, surface Chl *a* concentration was significantly higher at the cyclonic eddy stations ((0.204±0.001) μg/L) and was lower at the anticyclonic eddy stations ((0.112±0.023) μg/L) as compared with that at the reference stations (*t*-test, $p<0.05$; Table 1). The average concentration of Chl *a* in the upper 100 m was significantly higher at the cyclonic eddy stations ((0.202±0.003) μg/L), while it was significantly lower at the anticyclonic eddy stations ((0.115±0.023) μg/L; *t*-test, $p<0.01$; Fig. 3a; Table 1). Due to upwelling in the cyclonic eddy and downwelling in the anticyclonic eddy, the depth of Chl *a* maximum (DCM) at the cyclonic eddy, anticyclonic eddy and reference stations were 25, 75 and 50 m, respectively (Fig. 2e). The average integrated primary production in the euphotic zone was significantly higher at the cyclonic eddy stations, while it was significantly lower at the anticyclonic eddy stations as compared with that at the reference stations (*t*-test, $p<0.05$; Table 1).

The average concentration of silicate was low in the surface

Table 1. The average values of temperature, salinity, silicate, reactive Al, Chl *a* and integrated primary production (IPP) in the upper 100 m water column at cyclonic eddy (n=3), anticyclonic eddy (n=10) and reference (n=18) stations

	Cyclonic eddy stations	Anticyclonic eddy stations	Reference stations
Temperature/°C	18.58±0.48**	22.48±0.44**	21.45±0.76
Salinity	34.32±0.05**	34.03±0.05**	34.14±0.06
Silicate/μmol·L^{-1}	10.2±1.9**	3.9±1.2**	5.4±1.3
Al/nmol·L^{-1}	137±7*	174±26	180±21
Chl *a*/μg·L^{-1}	0.202±0.003**	0.112±0.023**	0.141±0.032
IPP/mg·m^{-2}·d^{-1}	537±26*	314±58*	432±93

Note: The data is expressed as mean±standard deviation. ** and * indicate the *t*-test significant difference between the examined stations and the reference stations at the levels of 0.01 and 0.05, respectively.

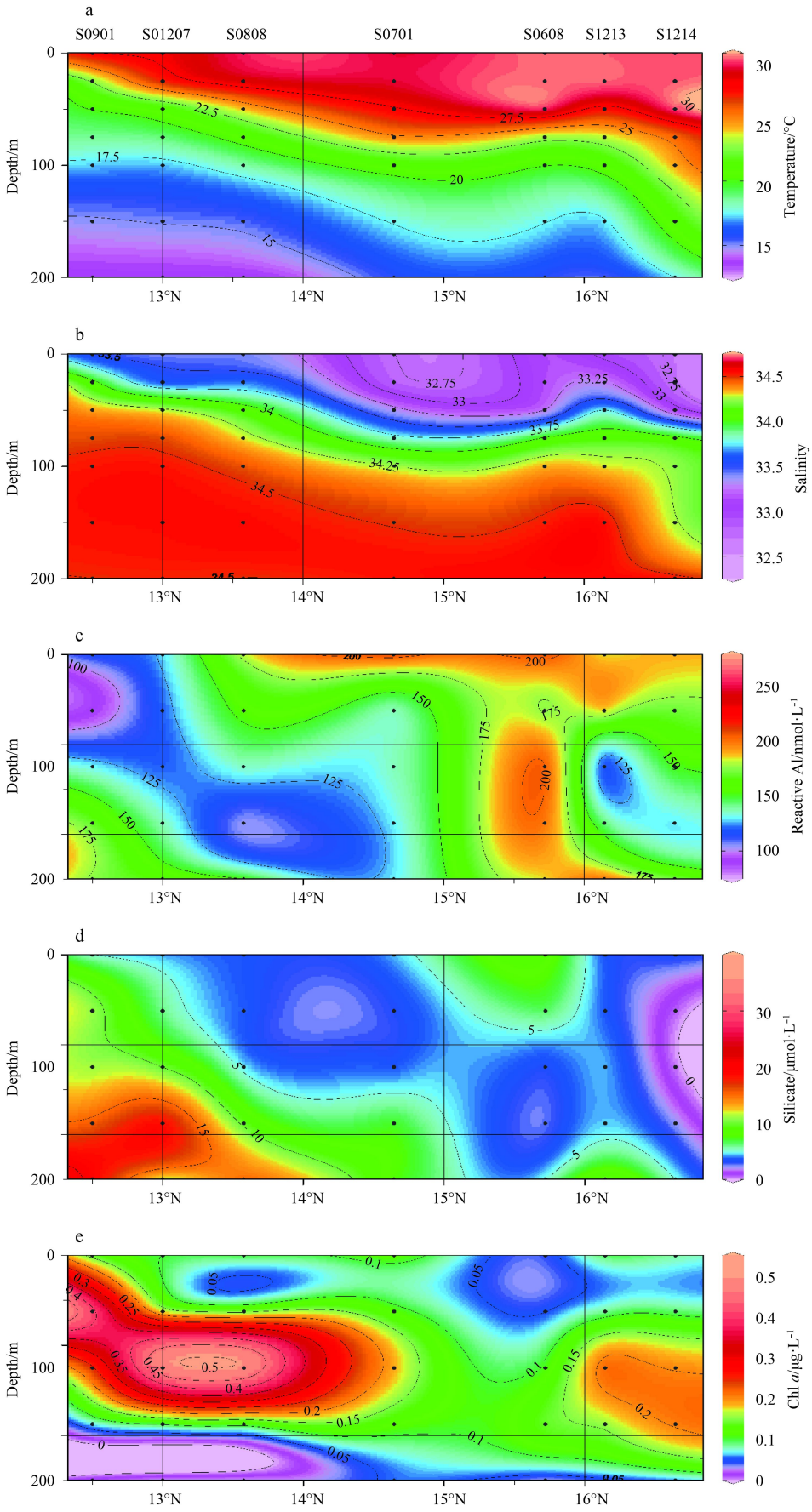

Fig. 2. Vertical profiles of temperature (a), salinity (b), reactive Al (c), silicate (d), and Chl *a* (e) in the upper water along Transect A.

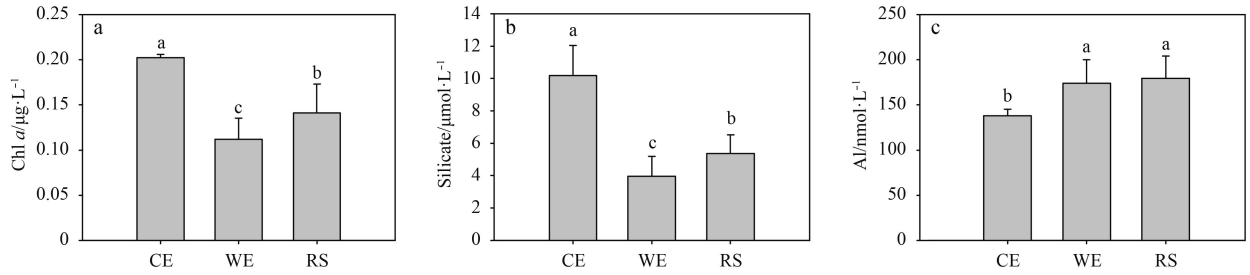

Fig. 3. Averaged Chl *a* (a), silicate (b) and reactive Al (c) in the upper 100 m water column for the cyclonic eddy (CE), anticyclonic eddy (WE) and reference stations (RS). Different lower letters above the error bar indicate significant difference (*t*-test, $p<0.05$). The error bar represents standard deviation.

water ((5.3±3.9) μmol/L) and reached to a minimum ((3.8±2.8) μmol/L) in the subsurface water, and then increased with the depth. The average concentration of silicate in the upper 100 m water column was significantly higher at the cyclonic eddy stations ((10.2±1.9) μmol/L), and lower at the anticyclonic eddy stations ((3.9±1.2) μmol/L; *t*-test, $p<0.01$; Fig. 3b; Table 1). The 10 μmol/L silicate isoline dramatically sank to the depth of 100 m at the anticyclonic eddy stations like S1214, while it was uplifted to the depth of 25 to 50 m at the cyclonic eddy stations like S0901, and was at near 75 m in depth at the reference stations (Fig. 2d).

3.4 *Distribution of reactive Al*

The concentration of reactive Al in the upper 200 m water column ranged from 58 nmol/L to 337 nmol/L in this study. Reactive Al in surface seawater ranged from 77 nmol/L to 328 nmol/L with a mean of (180±64) nmol/L, and and it did not significantly vary among the cyclonic eddy, anticyclonic eddy and reference stations (*t*-test, $p>0.05$). Generally, the reactive Al concentration reached to the maximum in the surface waters ((180±64) nmol/L), and decreased to the minimum in the subsurface waters and then increased again with the depth. Compared with those at the reference and anticyclonic eddy stations, the average concentration of reactive Al in the upper 100 m water column was significantly lower in the cyclonic eddy ((137±7) nmol/L; *t*-test, $p<0.05$; Fig. 3c; Table 1). The maximum average concentration of reactive Al in the upper 100 m water column (225 nmol/L) was observed at Sta. S0608 in the anticyclonic eddy (Fig. 2c).

The vertically minimum concentration of reactive Al occurred at the DCM at most of the stations (Figs 2c and e). For example, the minimum reactive Al concentration was 86 nmol/L at 25 m (DCM) at typical cyclonic eddy stations like S0901, and 155 nmol/L at 75 m (DCM) at typical anticyclonic eddy stations like S1214, and 94 nmol/L at 50 m (DCM) at reference stations like S0808 (Fig. 4).

4 Discussion

4.1 *Comparison of Al concentration with other regions*

Since samples in the present study were neither filtered nor pre-acidified, the reactive Al consisted of two fractions including fraction of the dissolved Al and fraction of the labile particulate Al (Al in particulate form that could be extracted by HAc, i.e., the so-called HAc-Al). By using a small subset of seawater samples collected from the cruise, we compared the measured Al concentrations between our unfiltered and unacidified samples and the filtered (0.2 μm) and acidified (HCl, pH=2) samples according to the method in Zhang et al. (2000) and Ren et al. (2011). The results demonstrated that the concentration of reactive Al (in unfiltered and unacidified samples) was 80%–95% of that of dissolved Al (in filtered and acidified samples) (Table 2). Therefore, we could use this ratio to estimate dissolved Al in this study and the estimated concentration of dissolved Al ranged from 61–421 nmol/L (corresponding to 58–337 nmol/L reactive Al). As contamination may introduced during the filtering and acidifying of the samples, dissolved Al measured in the filtered and acidified samples could be overestimated, therefore, the estimated concentrations of dissolved Al based on the reactive Al in this study could be overestimated.

Numerous studies have reported on the Al distributions in many oceans, but there are few studies on the distribution of Al in the SCS. To our knowledge, only two publications to date have documented Al distribution in this region. By using lumogallion fluorescence detection (Obata et al., 2000), Obata et al. (2004) reported that the dissolved Al in the upper 100 m column in the central basin of SCS ranged from 11.1 to 33.7 nmol/L. However, only one station (15.22°N, 115.17°E) was sampled in their study, and the seawater for the measurement of dissolved Al was filtered through a filter with a pore size of 0.04 μm, not the filters with a pore size of 0.45 μm/0.2 μm, the frequently-used sizes for measuring dissolved Al. Using filters with a smaller pore size might result in the relatively lower values. With samples filtered by acetate filters with a pore size of 0.45 μm, Wang et al. (2014) reported that the concentration of dissolved Al in the upper layer of the central and southern South China Sea ranged from 89 to 202 nmol/L (0.45 μm filtered) using the Al-lumogallion method described by Zhang et al. (2000) and Ren et al. (2011). Our estimated dissolved Al concentration (61–421 nmol/L) in the western SCS is consistent with the published values of dissolved Al from 37 to 178 nmol/L in the upper layer of Mediterranean using electron capture detector-gas chromatography (Measures and Edmond, 1988), 23–657 nmol/L (unfiltered) in the surface samples of Arabian Sea using the Pyrocatechol Violet spectrophotometric method of Koroleff (Narvekar and Singbal, 1993), 23–288 nmol/L in the Bohai Sea (Ren et al., 2002), 13–88 nmol/L (0.45 μm filtered) and 11–99 nmol/L (0.45 μm filtered) in the Yellow Sea and East China Sea (Li et al., 2008) using the Al-lumogallion method (Zhang et al., 2000; Ren et al., 2011), respectively.

Besides the potential overestimation of the dissolved Al, high atmospheric deposition might be another possible reason for the high dissolved Al concentration in the studied waters. Atmospheric dust input has been recognized the main source of Al in the upper layer of open oceans (Duce et al., 1991; Measures and Vink, 2000; Kramer et al., 2004). It has been reported that high amount of atmospheric dust (as much as 67 Tg/a) originated from Asia inland desert is deposited in the SCS (Zhang et al., 1993; Arimoto et al., 1997; Wang et al., 2012; Chuang et al., 2013). The dust deposition brings not only macronutrients and iron, but also substantial other trace metals, such as Al (Duce et al., 1991;

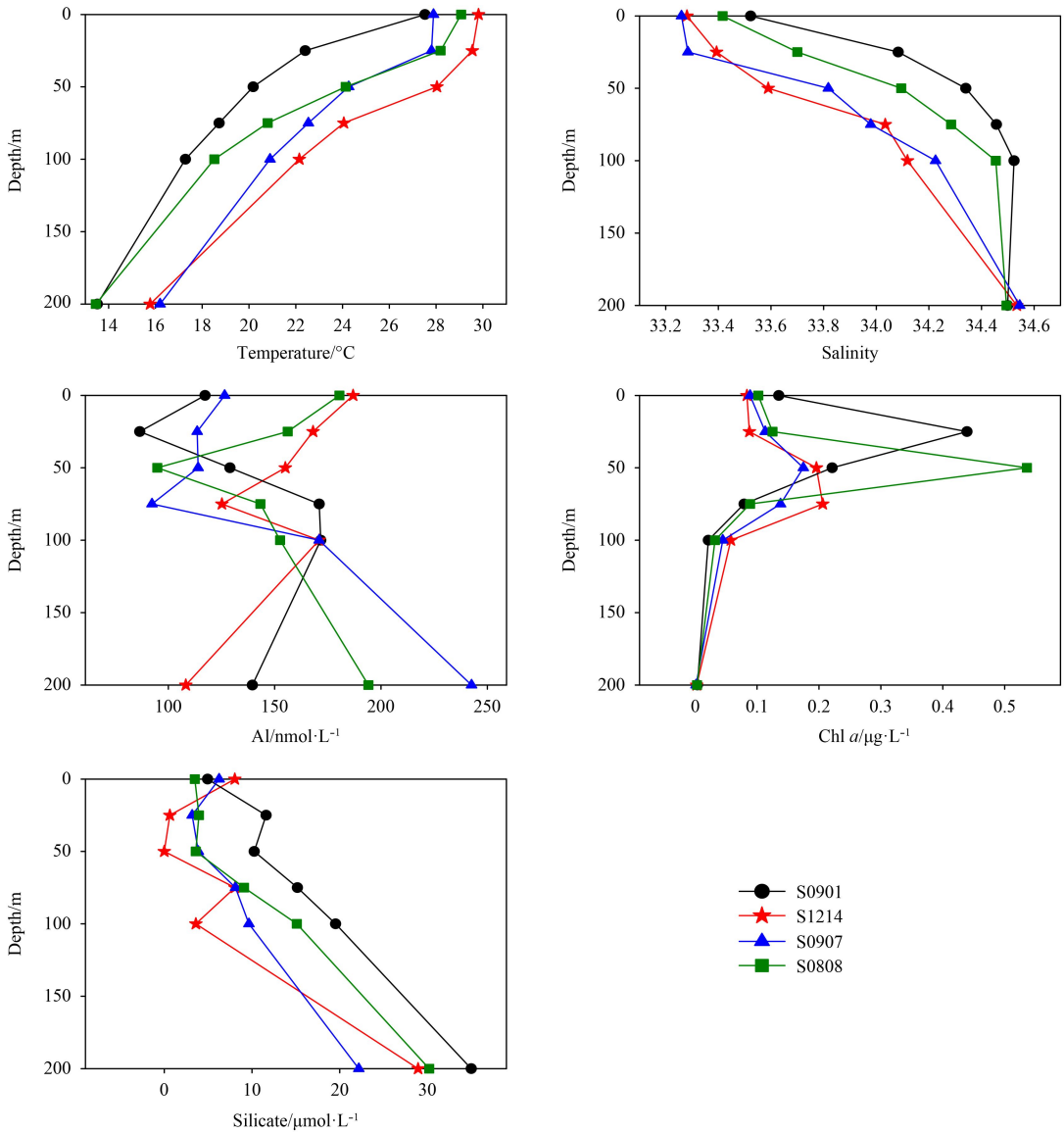

Fig. 4. Examples of vertical profiles of temperature, salinity, silicate, reactive Al and Chl *a* at typical stations. S0901 is a typical cyclonic eddy station, S1214 a typical anticyclonic eddy station, and S0907 and S0808 reference stations.

Table 2. The comparison values of Al between the unfiltered and unacidified samples (reactive Al) and the filtered (0.2 μm) and acidified (HCl, pH=2) samples (dissolved Al) from a small subset of seawater samples

Sample	Dissolved Al/nmol·L^{-1}	Reactive Al/nmol·L^{-1}	Reactive/dissolved ratio/%
1	134±5	107±12	80.07
2	92±6	86±3	93.87
3	64±5	57±6	89.58
4	75±9	61±6	81.09
5	176±4	153±4	86.96
6	233±9	218±11	93.84
7	306±14	277±12	90.32
8	82±7	67±8	81.71

Note: The data is expressed as mean±standard deviation (n=3).

Uematsu et al., 2002, 2003; Cohen et al., 2004; Paytan et al., 2009; Ho et al., 2010).

4.2 *Biological removal of Al in the western SCS*

Substantial studies have shown that biological removal is an important factor influencing the distribution of Al in seawater (Stoffyn, 1979; Ren et al., 2011; Li et al., 2013). Possible biological removal processes include active biological uptake of Al into phytoplankton cells (Stoffyn and Mackenzie, 1982; Chou and Wollast, 1997; Gehlen et al., 2002, 2003), and passive absorption of Al onto biogenic particles (Moran and Moore, 1992; Measures and Vink, 2000).

The vertical distribution of reactive Al, including decreasing from the highest concentration of reactive Al in surface water to the subsurface minima close to the Chl a maxima and then increasing of the reactive Al again with the Chl *a* decreasing below the DCM in this study (Figs 2c and 4), is in line with the results observed in the Atlantic Ocean (Dammshäuser et al., 2013), and indicates that the reactive Al in the upper water column was significantly influenced by biological removal processes such as biological uptake, and passive adsorption on biogenic particle surface. In addition, the significant negative correlation between the concentrations of reactive Al and Chl *a* in the upper 100 m water column (r=–0.718, p<0.01) further indicate significant biological scavenging of Al in this region (Fig. 5).

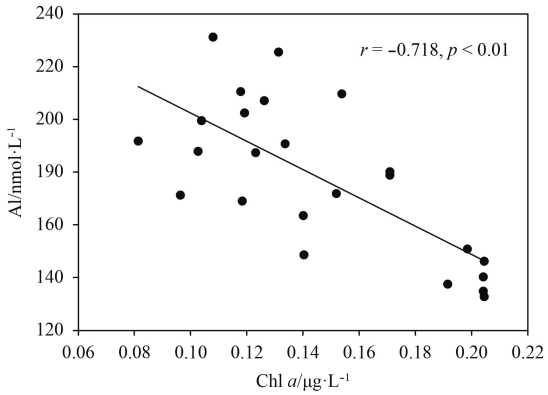

Fig. 5. Relationship between reactive Al and Chl *a* in the upper 100 m water column in the western SCS during August 9 to 29, 2013.

4.3 *Eddies regulated the reactive Al distribution through influencing biological removal*

It has been reported that mesoscale eddy can impact nutrient supply and primary production, and shift phytoplankton community in the euphotic zone (McGillicuddy et al., 1998; Benitez-Nelson et al., 2007). Our results suggest that mesoscale eddies could regulate the distribution of reactive Al by (1) influencing the primary production and (2) phytoplankton community structure, which are associated with the biological removal efficiency of Al in seawater (Figs 3a and c).

Mesoscale eddies could affect the distribution of reactive Al by regulating the primary production. In this study, the average Chl *a* in the cyclonic eddy stations was 43.3% higher than that of the reference stations, while it was about 20.6% less in the anticyclonic eddy stations. The increased Chl *a* concentration in the cyclonic eddy (Fig. 3a) indicates that deep-water upwelling and uplift of the nutricline in the cyclonic eddy (Figs 2a, b and d) could supply nutrients into the nutrient-depleted euphotic zone, and effectively stimulate the phytoplankton growth and primary production there (Hu et al., 2014). The high phytoplankton biomass indicates potentially high particle scavenging in the cyclonic eddy-affected waters (Ren et al., 2011; Li et al., 2013). The potential high biogenic particle flux indicated by the high primary production occurred in the cyclonic eddy (Table 1), would scavenge much dissolved Al from the water column (Narvekar and Singbal, 1993) and result in low dissolved Al there. So it is no wonder that a lower concentration of Al and higher concentration of Chl *a* were observed in the cyclonic eddy (Figs 3a and c). By contrast, surface-water downwelling could block nutrient supplement from the deeper layer to the surface, and consequently led to low Chl *a* (Fig. 3a) and low biological removal of Al in the anticyclonic eddy. Thus it is not surprising that the maximum concentration of reactive Al occurred at Sta. S0608 in the anticyclonic eddy characterized with low phytoplankton biomass (Chl *a*) (Figs 2c and e). The mean radius of the cyclonic and anticyclonic eddies in this area was around 280 km with a typical lifetime about three months based on the data from over the past 15 years (1993–2007) (Chen, 2010). In addition, numerous mesoscale eddies were always persistently found in the SCS. On average, there were about 32.8±3.4 eddies (Xiu et al., 2010), with a radius of around 150 km and a lifetime about 130 days (Wang et al., 2003), and the mean area covered by these eddies each year was around 160 170 km^2, equivalent to 9.8% of the SCS area with water depths greater than 1 000 m (Xiu et al., 2010; Chow et al., 2008). It was reported that the averaged integrated primary production in cyclonic and anticyclonic eddies are about 29.5% higher and 16.6% lower than the total average in the SCS, respectively (Hu et al., 2014). Overall, mesoscale eddies are crucial physical processes that affect the biological primary production and trace metal such as Al in the SCS.

The biological scavenging of Al could also be affected by shift in phytoplankton community structure influenced by mesoscale eddies. Previous studies showed that the diatom to dinoflagellate ratio significantly increased in the cyclonic eddy and decreased in the anticyclonic eddy in the western SCS (Zhong et al., 2013), and nutrient supply in cyclonic eddy may even support a diatom bloom (Benitez-Nelson et al., 2007). In this study, the average concentration of silicate in the cyclonic eddy stations was 88.9% higher than that of the reference stations, while it was about 27.8% less in the anticyclonic eddy stations. The relatively higher silicate concentration in the cyclonic eddy and lower concentration in the anticyclonic eddy observed in the present study (t-test, p<0.05; Fig. 3b), may support a higher diatom to dinoflagellate ratio in the cyclonic eddy and a lower value in the anticyclonic eddy. It has been reported that diatoms could scavenge Al more effectively than dinoflagellates (Chou and Wollast, 1997; Gehlen et al., 2002; Li et al., 2013; Wang et al., 2013). Ultimately, the different scavenging abilities between diatoms and dinoflagellates may contribute to the lower reactive Al in the cyclonic eddy stations while higher reactive Al in the anticyclonic eddy stations.

So far, only few studies have reported the link between the distribution of Al and mesoscale eddy. Gelado-Caballero et al. (1996) found that anticylonic eddy sank Al-depleted surface waters while the cyclonic eddy upwelled Al-enriched deep water in the Central East Atlantic waters. They argued that the small increase in primary production induced by cyclonic eddy does not seem to be sufficient to efficiently remove Al compared to the upwelling waters, where dissolved Al was scavenged. Brown et al. (2012) reported that Al was elevated in anticyclonic eddy core waters compared to basin stations in the northern Gulf of Alaska due to the riverine discharge-influenced coastal water along the shelf. The present study is the first reporting Al data related to mesoscale eddies in the SCS. We found a significant negative correlation between the average concentrations of reactive Al and Chl *a* in the upper 100 m water column, suggesting that the reactive Al in the upper water column was significantly influenced by biological removal processes.

5 Conclusions

Our results indicate that mesoscale eddies could regulate the

distribution of reactive Al by influencing the primary production and phytoplankton community structure in the western SCS. Our study is the first reporting Al data related to mesoscale eddies in the SCS. The vertical distribution of reactive Al and the negative correlation between reactive Al and Chl *a* both suggest that the reactive Al in the upper water column was significantly influenced by biological removal processes. Overall, mesoscale eddies are crucial physical processes that affect the biological primary production and trace meatal such as Al in the SCS.

Acknowledgements

The authors are grateful to Wang Junxing for helpful discussion during the preparation of this manuscript. We also appreciate the support from the captain and crews of the R/V *Shiyan III*.

References

Arimoto R, Gao Y, Zhou M Y, et al. 1997. Atmospheric deposition of trace elements to the Western Pacific basin. In: Baker J E, ed. Atmospheric Deposition of Contaminants to the Great Lakes and Coastal Waters. Florida: SETAC Press, 209–225

Behrenfeld M J, Falkowski P G. 1997. Photosynthetic rates derived from satellite-based chlorophyll concentration. Limnol Oceanogr, 42(1): 1–20

Benitez-Nelson C R, Bidigare R R, Dickey T D, et al. 2007. Mesoscale eddies drive increased silica export in the subtropical Pacific Ocean. Science, 316(5827): 1017–1021

Berger C J, Lippiatt S M, Lawrence M G, et al. 2008. Application of a chemical leach technique for estimating labile particulate aluminum, iron, and manganese in the Columbia River plume and coastal waters off Oregon and Washington. J Geophys Res, 113(C2): doi: 10.1029/2007JC004703

Brown M T, Lippiatt S M, Lohan M C, et al. 2012. Trace metal distributions within a Sitka eddy in the northern Gulf of Alaska. Limnol Oceanogr, 57(2): 503–518

Chen Gengxin. 2010. Mesoscale eddies in the South China Sea: mean properties and spatio-temporal variability (in Chinese) [dissertation]. Beijing: University of Chinese Academy of Sciences

Chou L, Wollast R. 1997. Biogeochemical behavior and mass balance of dissolved aluminum in the western Mediterranean Sea. Deep Sea Res II, 44(3–4): 741–768

Chow C H, Hu J H, Centurioni L R, et al. 2008. Mesoscale Dongsha Cyclonic Eddy in the northern South China Sea by drifter and satellite observations. J Geophys Res, 113(C4): C04018

Chuang M T, Chang S C, Lin N H, et al. 2013. Aerosol chemical properties and related pollutants measured in Dongsha Island in the northern South China Sea during 7-SEAS/Dongsha Experiment. Atmos Environ, 78: 82–92

Cohen D D, Garton D, Stelcer E, et al. 2004. Multielemental analysis and characterization of fine aerosols at several key ACE-Asia sites. J Geophys Res, 109(D19): D19S12

Dammshäuser A, Wagener T, Croot P L. 2011. Surface water dissolved aluminum and titanium: tracers for specific time scales of dust deposition to the Atlantic. Geophys Res Lett, 38(24): L24601

Dammshäuser A, Wagener T, Garbe-Schönberg D, et al. 2013. Particulate and dissolved aluminum and titanium in the upper water column of the Atlantic Ocean. Deep Sea Res I, 73: 127–139

Duce R A, Liss P S, Merrill J T, et al. 1991. The atmospheric input of trace species to the world ocean. Global Biogeochem Cycles, 5(3): 193–259

Gehlen M, Beck L, Calas G, et al. 2002. Unraveling the atomic structure of biogenic silica: evidence of the structural association of Al and Si in diatom frustules. Geochim Cosmochim Acta, 66(9): 1601–1609

Gehlen M, Heinze C, Maier-Reimer E, et al. 2003. Coupled Al-Si geochemistry in an ocean general circulation model: a tool for the validation of oceanic dust deposition fields. Global Biogeochem Cycles, 17(1): 1028

Gelado-Caballero M D, Torres-Padrón M E, Hernández-Brito J J, et al. 1996. Aluminium distributions in Central East Atlantic waters (Canary Islands). Mar Chem, 51(4): 359–372

Giesbrecht T, Sim N, Orians K J, et al. 2013. The distribution of dissolved and total dissolvable aluminum in the Beaufort Sea and Canada Basin region of the Arctic Ocean. J Geophys Res, 118(12): 6824–6837

Han Qin, Moore J K, Zender C, et al. 2008. Constraining oceanic dust deposition using surface ocean dissolved Al. Global Biogeochem Cycles, 22(2): GB2003

Ho T Y, Chou W C, Wei C L, et al. 2010. Trace metal cycling in the surface water of the South China Sea: vertical fluxes, composition, and sources. Limnol Oceanogr, 55(5): 1807–1820

Hu Zifeng, Tan Yehui, Song Xingyu, et al. 2014. Influence of mesoscale eddies on primary production in the South China Sea during spring inter-monsoon period. Acta Oceanol Sin, 33(3): 118–128

Hydes D J. 1989. Seasonal variation in dissolved aluminium concentrations in coastal waters and biological limitation of the export of the riverine input of aluminium to the deep sea. Cont Shelf Res, 9(10): 919–929

Hydes D J, de Lange G J, de Baar H J W. 1988. Dissolved aluminium in the Mediterranean. Geochim Cosmochim Acta, 52(8): 2107–2114

Kirkwood D S, Aminot A, Carlberg S. 1996. The 1994 quasimeme laboratory performance study: nutrients in seawater and standard solutions. Mar Pollut Bull, 32(8–9): 640–645

Kramer J, Laan P, Sarthou G, et al. 2004. Distribution of dissolved aluminium in the high atmospheric input region of the subtropical waters of the North Atlantic Ocean. Mar Chem, 88(3–4): 85–101

Li Faming, Ren Jingling, Yan Li, et al. 2013. The biogeochemical behavior of dissolved aluminum in the southern Yellow Sea: influence of the spring phytoplankton bloom. Chin Sci Bull, 58(2): 238–248

Li Jianbing, Ren Jingling, Zhang Jing, et al. 2008. The distribution of dissolved aluminum in the Yellow and East China Seas. J Ocean Univ China, 7(1): 48–54

McGillicuddy D J, Robinson A R, Siegel D A, et al. 1998. Influence of mesoscale eddies on new production in the Sargasso Sea. Nature, 394(6690): 263–266

Measures C I. 1999. The role of entrained sediments in sea ice in the distribution of aluminium and iron in the surface waters of the Arctic Ocean. Mar Chem, 68(1–2): 59–70

Measures C I, Brown M T, Vink S. 2005. Dust deposition to the surface waters of the western and central North Pacific inferred from surface water dissolved aluminum concentrations. Geochem Geophys Geosyst, 6(9): doi: 10.1029/2005GC000922

Measures C I, Edmond J M. 1988. Aluminum as a tracer of the deep outflow from the Mediterranean. J Geophys Res, 93(C1): 591–595

Measures C I, Edmond J M. 1990. Aluminium in the South-Atlantic: steady-state distribution of a short residence time element. J Geophys Res, 95(C4): 5331–5340

Measures C I, Hatta M, Fitzsimmons J, et al. 2015. Dissolved Al in the zonal N Atlantic section of the US GEOTRACES 2010/2011 cruises and the importance of hydrothermal inputs. Deep Sea Res II, 116: 176–186

Measures C I, Vink S. 2000. On the use of dissolved aluminum in surface waters to estimate dust deposition to the ocean. Global Biogeochem Cycles, 14(1): 317–327

Moore R M. 1981. Oceanographic distributions of zinc, cadmium, copper and aluminium in waters of the central arctic. Geochim Cosmochim Acta, 45(12): 2475–2482

Moran S B, Moore R M. 1988. Evidence from mesocosm studies for biological removal of dissolved aluminium from sea water. Nature, 335(6192): 706–708

Moran S B, Moore R M. 1992. Kinetics of the removal of dissolved aluminum by diatoms in seawater: a comparison with thorium. Geochim Cosmochim Acta, 56(9): 3365–3374

Narvekar P V, Singbal S Y S. 1993. Dissolved aluminium in the surface microlayer of the Eastern Arabian Sea. Mar Chem, 42(2):

85–94
Obata H, Nozaki Y, Okamura K, et al. 2000. Flow-through analysis of Al in seawater by fluorometric detection with the use of lumogallion. Field Anal Chem Technol, 4(6): 274–282
Obata H, Nozaki Y, Alibo D S, et al. 2004. Dissolved Al, In, and Ce in the eastern Indian Ocean and the Southeast Asian Seas in comparison with the radionuclides ^{210}Pb and ^{210}Po. Geochim Cosmochim Acta, 68(5): 1035–1048
Orians K J, Bruland K W. 1986. The biogeochemistry of Aluminum in the Pacific-Ocean. Earth Planet Sci Lett, 78(4): 397–410
Parsons T R, Maita Y, Lalli C M. 1984. A Manual of Chemical and Biological Methods for Seawater Analysis. New York: Pergamon Press, 475–490
Paytan A, Mackey K R M, Chen Ying, et al. 2009. Toxicity of atmospheric aerosols on marine phytoplankton. Proc Natl Acad Sci U SA, 106(12): 4601–4605
Ren Jingling, Zhang Jing, Luo Jingqing, et al. 2001. Improved fluorimetric determination of dissolved aluminium by micelle-enhanced lumogallion complex in natural waters. Analyst, 126(5): 698–702
Ren Jingling, Zhang Jing. 2002. Studies on marine biogeochemistry of aluminum. Marine Environmental Science (in Chinese), 21(1): 68–74
Ren Jingling, Zhang Guoling, Zhang Jing, et al. 2011. Distribution of dissolved aluminum in the Southern Yellow Sea: Influences of a dust storm and the spring bloom. Mar Chem, 125(1–4): 69–81
Schüßler U, Balzer W, Deeken A. 2005. Dissolved Al distribution, particulate Al fluxes and coupling to atmospheric Al and dust deposition in the Arabian Sea. Deep Sea Res II, 52(14–15): 1862–1878
Stoffyn M. 1979. Biological control of dissolved aluminum in seawater: experimental evidence. Science, 203(4381): 651–653
Stoffyn M, Mackenzie F T. 1982. Fate of dissolved aluminum in the oceans. Mar Chem, 11(2): 105–127
Taylor S R. 1964. Trace element abundances and the chondritic earth model. Geochim Cosmochim Acta, 28(12): 1989–1998
Tria J, Butler E C V, Haddad P R, et al. 2007. Determination of aluminium in natural water samples. Anal Chim Acta, 588(2): 153–165
Uematsu M, Wang Zifa, Uno I. 2003. Atmospheric input of mineral dust to the western North Pacific region based on direct measurements and a regional chemical transport model. Geophys Res Lett, 30(6): 1342
Uematsu M, Yoshikawa A, Muraki H, et al. 2002. Transport of mineral and anthropogenic aerosols during a Kosa event over East Asia. J Geophys Res, 107(D7): AAC 3-1–AAC 3–7
Wang S H, Hsu N C, Tsay S C, et al. 2012. Can Asian dust trigger phytoplankton blooms in the oligotrophic northern South China Sea. Geophys Res Lett, 39(5): L05811
Wang Zhaowei, Ren Jingling, Yan Li, et al. 2013. Preliminary study on scavenging mechanism of dissolved aluminum by phytoplankton. Acta Ecol Sin (in Chinese), 33(22): 7140–7147
Wang Guihua, Su Jilan, Chu P C. 2003. Mesoscale eddies in the South China Sea observed with altimeter data. Geophys Res Lett, 30(21): 2121
Wang Qiong, Tan Yehui, Zhou Linbin, et al. 2014. Research on dissolved aluminum in the central and southern South China Sea: can aluminum stimulate Pyrrophyta's growth. J Trop Oceanogr (in Chinese), 33(2): 78–86
Xiu Peng, Chai Fei, Shi Lei, et al. 2010. A census of eddy activities in the South China Sea during 1993–2007. J Geophys Res, 115(C3): C03012
Xue Huijie, Chai Fei, Pettigrew N, et al. 2004. Kuroshio intrusion and the circulation in the South China Sea. J Geophys Res, 109(C2): C02017
Zhang J, Liu Sumei, Lü X, et al. 1993. Characterizing Asian wind-dust transport to the Northwest Pacific Ocean. Direct measurements of the dust flux for two years. Tellus B, 45(4): 335–345
Zhang Jing, Xu H, Ren Jingling. 2000. Fluorimetric determination of dissolved aluminium in natural waters after liquid-liquid extraction into n-hexanol. Anal Chim Acta, 405(1–2): 31–42
Zhong Chao, Xiao Wupeng, Huang Bangqin. 2013. The response of phytoplankton to mesoscale eddies in the western South China Sea. Advances in Marine Science (in Chinese), 31(2): 213–220